Atmos. Meas. Tech. Discuss., 3, 1323–1359, 2010
www.atmos-meas-tech-discuss.net/3/1323/2010/

Atmospheric Measurement Techniques Discussions

This discussion paper is/has been under review for the journal Atmospheric Measurement Techniques (AMT). Please refer to the corresponding final paper in AMT if available.

Synergy between CALIOP and MODIS instruments for aerosol monitoring: application to the Po Valley

P. Royer[1,2], **J.-C. Raut**[3,*], **G. Ajello**[1], **S. Berthier**[1,**], **and P. Chazette**[1,3]

[1]Laboratoire des Sciences du Climat et de l'Environnement (LSCE), Laboratoire mixte CEA-CNRS-UVSQ, UMR 1572, CEA Saclay, 91191 Gif-sur-Yvette, France
[2]LEOSPHERE, 76 rue de Monceau, 75008 Paris, France
[3]Laboratoire de Météorologie Dynamique (LMD), UMR 8539, Ecole Polytechnique, 91128 Palaiseau, France
[*]now at: Laboratoire Atmosphères Milieux Observations Spatiales (LATMOS), Laboratoire mixte CNRS-UVSQ-UPMC, UMR 8190, Université Paris 6, 4 Place Jussieu 75252 Paris, France
[**]now at: Koninklijk Nederlands Meteorologisch Instituut (KNMI), De Bilt, The Netherlands

Received: 10 February 2010 – Accepted: 23 March 2010 – Published: 29 March 2010

Correspondence to: P. Royer (philippe.royer@lsce.ipsl.fr)

Published by Copernicus Publications on behalf of the European Geosciences Union.

Abstract

We propose here a synergy between Cloud-Aerosol Lidar and Infrared Pathfinder Satellite Observations/Cloud-Aerosol LIdar with Orthogonal Polarization (CALIPSO/CALIOP) and Moderate Resolution Imaging Spectroradiometer (MODIS) onboard Aqua and Terra in order to retrieve aerosol optical properties over the Po Valley from June 2006 to February 2009. Such an approach gives simultaneously access to the aerosol extinction vertical profile and to the equivalent backscatter-to-extinction ratio at 532 nm (BER, inverse of the lidar ratio). The choice of the Po valley has been driven by the great occurrences of pollutant events leading to a mean MODIS-derived aerosol optical thickness of 0.27(±0.17) at 550 nm over a large area of ~120 000 km^2. In such area, a significant number of CALIOP level-1 vertical profiles can be averaged (~200 individual laser shots) leading to a signal-to-noise ratio greater than 10 in the planetary boundary layer (PBL) sufficient to perform a homemade inversion of the mean lidar profiles. The mean BER (together with the associated variabilities) over the Po Valley retrieved from the coupling between CALIOP/MODIS-Aqua and CALIOP/MODIS-Terra are ~0.014(±0.003) sr^{-1} and ~0.013(±0.004) sr^{-1}, respectively. The total uncertainty on BER retrieval has been assessed to be ~0.003 sr^{-1} using a Monte Carlo approach. These mean BER values retrieved have been compared with those given by the level-2 operational products of CALIOP ~0.016(±0.003) sr^{-1}. The values we assessed appear close to what is expected above urban area. A seasonal cycle has been observed with higher BER values in spring, summer and fall, which can be associated to dust event occurring during this period. In most of cases, the mean aerosol extinction coefficient in the PBL diverges significantly between the level-2 operational products and the result of our own inversion procedure. Indeed, mean differences of 0.10 km^{-1} (~50%) and 0.13 km^{-1}(~60%) have been calculated using MODIS-Aqua/CALIOP and MODIS-Terra/CALIOP synergies, respectively. Such differences may be due to the identification of the aerosol model by the operational algorithm and thus to the choice of the BER.

1 Introduction

Aerosol pollution study in the greatest urban centers is of increasing interest as it directly concerns half of the world population. Moreover, a continuous development of huge cities in the future 40 years would constrain two thirds of the world population to live into megalopolis or close to industrial areas. Now, it has been clearly established that small particles with a radius lower than 2.5 µm ($PM_{2.5}$) increase cardiovascular troubles (e.g. Dockery and Pope, 1996; Lauwerys et al., 1982). Several studies have also shown that megalopolis had a regional impact on air quality and climate (e.g. Lawrence et al., 2007). The study of these areas is thus important to improve our understanding of physical and chemical processes that play a key role on pollution peaks. This will help improving chemistry-transport models, defining more accurate scenarios of emission mitigation and improving the forecast of pollution events.

The new generation of spaceborne missions is a new insight to follow pollution levels over the whole atmosphere and over specific areas where human activities have significantly modified the natural equilibrium. The synergy between active and passive remote sensing instruments is a powerful tool in atmospheric studies dedicated to the evaluation of human impact. The A-train Satellite Constellation (Afternoon Constellation) is a significant part of these new approaches and lets to consider the future spaceborne missions using instrumental synergy from space.

Instrumental synergies have already proved their ability to retrieve aerosol optical properties with a good accuracy. Ground-based synergies involving lidar and sunphotometer have been used in the framework of the INDian Ocean EXperiment (INDOEX) to determine aerosol optical properties (Chazette, 2003). A similar approach has been used in the Lidar pour la surveillance de l'AIR (LISAIR) program around Paris area (Raut and Chazette, 2007). During the African Multidisciplinary Monsoon Analysis (AMMA) campaign, the aerosol radiative budget has been assessed using airborne lidar and in situ measurements together with a ground-based sunphotometer (e.g. Raut and Chazette, 2008b; Haywood et al., 2008). During previous campaigns, the passive/active instrumental synergy has also been used onboard an aircraft (e.g. Pelon et al., 2002) or involving airborne and spaceborne measurements (e.g. Chazette et al., 2001; Dulac and Chazette, 2003). For the first time, a spaceborne synergy between Lidar in-Space Technology Experiment (LITE) and Meteosat has been used to determine dust properties over deserts (Berthier et al., 2006) and has thus shown the interest of such an approach.

Contrary to ground-based observations, spatial instruments allow global or regional scale approaches to deal with both air quality and climate issues. The Po Valley is a large European polluted area of ~120 000 km^2 oriented east-west with a mean width of ~100 km. It is then particularly suitable for spatial studies using the synergy between Cloud-Aerosol Lidar and Infrared Pathfinder Satellite Observations/Cloud-Aerosol LIdar with Orthogonal Polarization (CALIPSO/CALIOP) and Moderate Resolution Imaging Spectroradiometer onboard Aqua (MODIS-Aqua) and Terra (MODIS-Terra).

The Po valley is among the most polluted area in Western Europe. The presence of large cities, the high density of industries and population (more than 100 people per km^2), the presence of mountains surrounding this region (the Alps in the north and the west, and the Apennines in the south) concentrate the pollutants in the planetary boundary layer (PBL) and lead to a high aerosol loading particularly in summer with a mean optical thickness close to 0.4 at 550 nm (e.g. Barnaba and Gobbi, 2004). Figure 1 shows the topography and the location of the main cities in the Po valley. Many scientific studies and specific campaigns have been conducted in the Po Valley, such as Pianura Padana ozone production (PIPAPO; Neftel et al., 2002), Pollution hot-spot monitoring from GOME applied to the Po basin (POLPO; Petritoli et al., 2004), Quantification of aerosol nucleation in the European boundary layer (QUEST; Laaksonen et al., 2005) and Aerosol Direct Radiative Experiment (ADRIEX; Highwood et al., 2007).

In this paper we have performed a multiannual study involving a synergy between CALIOP and MODIS spaceborne instruments in order to retrieve the temporal evolution of aerosol optical properties over the Po Valley from June 2006 to February 2009. The main tools used in our study are presented in Sect. 2. The methodology is detailed in Sect. 3 and the results are described and discussed in Sect. 4.

2 Observations

2.1 CALIPSO/CALIOP lidar

CALIOP is a spaceborne nadir-pointing lidar launched on 28 April 2006 aboard CALIPSO satellite (http://www-calipso.larc.nasa.gov) to join the Afternoon Constellation (A-train, Stephens et al., 2002). Its 705 km-height sun-synchronous orbit flies over the same area every 16 days. The emission is based on a diode-pumped Nd:YAG producing linearly-polarized pulses of light at 1064 and 532 nm with a mean pulse energy of 110 mJ and a repetition rate of 20.25 Hz i.e. a horizontal resolution of 333 m (Winker et al., 2003). The receiver is composed of a 1-m telescope and three detectors to measure the backscattered signal at 1064 nm and the parallel and perpendicular components of the 532 nm return. The high vertical resolution of CALIOP lidar (30–60 m) provides information over land and ocean on optical, physical and structural properties of aerosols (e.g. Thomason et al., 2007; Kim et al., 2008) and clouds (e.g. Sassen et al., 2008; Berthier et al., 2008; Noel et al., 2008).

In this study, we have employed both the total attenuated backscatter coefficient at 532 nm (β^{att}) from CALIOP level-1 calibrated data product and the aerosol extinction (α_a) and backscatter (β_a) coefficients at 532 nm from level-2 aerosol products (http://eosweb.larc.nasa.gov/PRODOCS/calipso/table_calipso.html). Level-1 data have a high horizontal resolution (~0.3 km), whereas the level-2 data are given with a mean profile averaged over 40 km.

The CALIOP operational retrieval of α_a is computed using an aerosol backscatter-to-extinction ratio (BER, inverse of the so-called lidar ratio LR) determined with the selection algorithm described in the Scene Classification Algorithms (PC-SCI-202.03, Vaughan et al., 2004a) of the CALIOP Lidar Level II Algorithm Theoretical Basis

AMTD
3, 1323–1359, 2010

Document (ATBD). Aerosol extinction profiles are given with a vertical resolution of 120 m from the ground up to 8.2 km above the mean sea level (a.m.s.l.). Concerning the 40 km horizontal resolution aerosol products, the uncertainties on aerosol backscatter and extinction coefficients are respectively 20–30% and 40% assuming an uncertainty of 30% on BER (http://www-calipso.larc.nasa.gov/products/).

A total of 461 CALIPSO orbits have passed over the Po Valley between 13 June 2006 and 15 February 2009 at around 01:30 and 12:30 GMT for night-time and daytime tracks, respectively. Figure 1 represent CALIPSO orbits considered (yellow solid lines) and the portions considered with an altitude lower than 200 m (red solid lines). Among those 461 orbits only 121 (i.e. 26.25%) were obtained in cloud-free conditions. Each orbit has been connected with the nearest big city flew over by CALIPSO. Table 1 shows the apportionment of these orbits as a function of cities and seasons. This distribution is globally homogeneous in space and time, which is important so as to potentially determine a seasonal trend.

2.2 MODIS radiometers onboard TERRA and AQUA

Terra and Aqua Moderate Resolution Imaging Spectroradiometer (MODIS, Salmonson et al., 1989; King et al., 1992) have joined the A-train constellation on December 1999 and May 2002 respectively (http://modis.gsfc.nasa.gov). The polar orbit of Terra (http://terra.nasa.gov) passes over the equator from north to south in the morning, whereas Aqua (http://aqua.nasa.gov) has ascending node over the equator during the afternoon. The MODIS radiometers are composed of 36 spectral bands, or groups of wavelengths from 400 nm to 1440 nm. Their wide swaths of 110° (i.e. 2330 km) provide a global coverage of Earth's surface from one to two days with a resolution between 250 and 1000 m at ground level depending on the band.

We used here the aerosol optical depth (AOD) at 550 nm (τ_{MO}) from MODIS aerosol product level-2 data for Terra and Aqua platforms. Both products are given with a spatial resolution of 10×10 km^2 at nadir. The standard deviation on $\tau_{\mathrm{MO}i}$ retrieval over

AMTD
3, 1323–1359, 2010

land above the pixel i is $\sigma_{MOi} = \pm 0.05 \pm 0.2\tau_{MOi}$ (Chu et al., 2002). MODIS data are taken from June 2006 to February 2009.

2.3 AERONET sun-photometers

The AErosol RObotic NETwork (AERONET) is an automatic and global network of sun-photometers which provides long-term and continuous monitoring of aerosol optical, microphysical and radiative properties (http://aeronet.gsfc.nasa.gov/). Each site is composed of a sun and sky scanning spectral radiometer manufactured by CIMEL. For direct sun measurement eight spectral bands are used between 340 and 1020 nm. The five standard wavelengths are 440, 670, 870, 940 and 1020 nm. AOD data are computed for three data quality levels: level 1.0 (unscreened), level 1.5 (cloud-screened), and level 2.0 (cloud screened and quality-assured). The total uncertainty on AOD is $< \pm 0.01$ for $\lambda > 440$ nm and $< \pm 0.02$ for $\lambda < 440$ nm (Holben et al., 1998).

Three AERONET sun-photometers are located in the Po Valley at Modena, Ispra and Venice sites. We only used here level 2.0 data from Ispra station at 500 nm.

3 Method to retrieve the aerosol optical properties from the synergy between CALIOP and MODIS

Hereafter we present the methodology that we used to retrieve both the aerosol extinction coefficient and BER from the coupling between spaceborne CALIOP lidar system onboard CALIPSO and MODIS radiometers onboard Aqua or Terra. The corresponding retrievals will be further compared to the operational products.

AMTD

3, 1323–1359, 2010

Title Page

Abstract | Introduction

Conclusions | References

Tables | Figures

◀| |▶

◀ ▶

Back | Close

Full Screen / Esc

Printer-friendly Version

Interactive Discussion

3.1 MODIS-derived AOD constraint to solve the lidar equation

The total attenuated backscatter coefficient (β^{att}) against the distance s can be commonly written under the form (Measures, 1984):

$$\beta^{\text{att}}(s) = K\left(3/8\pi\,\alpha_m(s) + \text{BER}(s)\cdot\alpha_a(s)\right)\cdot\exp\left\{-2\int_0^s(\alpha_m(s')+\alpha_a(s'))\,ds'\right\} \tag{1}$$

K represents the system constant that is eliminated through normalization at an altitude where only molecular scattering occurs (so-called Rayleigh zone). The molecular scattering coefficient α_m can be determined from radiosoundings or climatic data of temperature and pressure so that only aerosol contributions are to determine. Hence, the lidar equation is an ill-posed problem requiring the retrieval of two unknowns: α_a and BER.

Different algorithms have been proposed to solve the previous equation using exogenous constraints or specific measurement geometries. BER can be i) estimated thanks to an a priori knowledge on the aerosol, or calculated ii) from multi-angular measurements (Sicard et al., 2002), iii) from the coupling between elastic and Raman channels (Ansmann et al., 1992), iv) from different geometries of lidar observations (Chazette et al., 2007) or v) from a synergy with a passive instrument measuring the total AOD as a sun-photometer (Chazette, 2003). The latter has been also successfully used considering the synergy between airborne lidar and Meteosat observations in Chazette et al. (2001) and in Dulac and Chazette (2003), and between the spaceborne lidar LITE and the geostationary satellite Meteosat in Berthier et al. (2006) to retrieve dust aerosol optical properties over ocean or continent. Here we consider the coupling between the passive instrument MODIS and the spaceborne lidar CALIOP. The method is based on the classical Klett (1981) algorithm and requires a dichotomous approach converging when the difference between CALIOP and MODIS-derived AOD is lower than 0.01. Such a value has been established for a relative residual error on BER lower than 3%.

The different sources of uncertainty on the lidar-derived aerosol extinction coefficient (α_a) are well described in Chazette et al. (1995). Uncertainties in the determination of α_a can be related to five main causes: (1) the statistical fluctuations in the measured signal, associated with random detection processes, (2) the uncertainty on the lidar signal in the altitude range used for the normalization, (3) the uncertainty on the a priori knowledge of the vertical profile of the molecular backscatter coefficient as determined from ancillary measurements, (4) the uncertainty on BER and on its altitude dependence, and (5) the overall uncertainty resulting from the value of τ_{MO} defined in Eq. (2).

An individual CALIOP level-1 profile is associated to a signal-to-noise ratio (SNR) in the PBL close to 1.5 (e.g. Berthier et al., 2008). It is not enough to retrieve the aerosol extinction profile. A significant part of the CALIPSO orbit has been therefore averaged in terms of lidar profiles. Regarding at topographic issues, the number of individual lidar profiles averaged depends on the orbit considered. This number has been reported in Table 1. The resulting SNR of the mean CALIOP profile is higher than 10 in the PBL after applying a low-pass filtering on the lidar data reducing the lidar vertical resolution to ~100 m. The lidar profiles have been calibrated to estimated molecular returns in a region deemed to be free from aerosols. SNR relative to the mean signal calculated on the Rayleigh zone has been calculated to be higher than 20. The uncertainty on the a priori knowledge of the molecular contribution has been assessed to be lower than 3% using a comparison between climatic mid-latitude and modeled vertical profiles of temperature. The uncertainty due to BER at 532 nm has been discussed in several papers (e.g. Raut and Chazette, 2008a). This is a major source of uncertainty depending on the constraint used. In the present paper, BER is considered constant with altitude. The effect of relative humidity on BER, which leads to both the aerosol radius growth and the modification of the complex refractive index, has been shown to be lower than 10% between RH=20% and 70% for urban aerosols at 532 nm (Raut and Chazette, 2008a).

AMTD

3, 1323–1359, 2010

Synergy between CALIOP and MODIS instruments

P. Royer et al.

The constraint brought by τ_{MO} needs to be representative of the considered part of the orbit. In this approach, it turns out to be the main error source. τ_{MO} has been calculated as the mean MODIS-derived AOD in a 10 km radius around the CALIPSO track. The individual AODs measured at pixel i ($\tau_{\mathrm{MO}i}$) have been weighted by the minimal distance d_i between the pixel centre and CALIPSO track, as:

$$\tau_{MO} = \frac{\sum_{i=1}^{p} d_i^{-1} \cdot \tau_{MOi}}{\sum_{i=1}^{p} d_i^{-1}} \tag{2}$$

with p the number of pixels taken into account in the vicinity of CALIPSO track.

With the reasonable assumption of statistical independence between pixels (i.e. $\tau_{\mathrm{MO}i}$ and $\tau_{\mathrm{MO}j}$ are independent for $i \neq j$), the standard deviation σ_{MO} on τ_{MO} is then given as a function of the individual standard deviations $\sigma_{\mathrm{MO}i}$ by:

$$\sigma_{\mathrm{MO}} = \sqrt{\frac{\sum_{i=1}^{p} d_i^{-2} \cdot \sigma_{\mathrm{MO}i}^2}{\left(\sum_{i=1}^{p} d_i^{-1}\right)^2}} \tag{3}$$

CALIPSO and Aqua or Terra are not exactly coincident in time. The aerosol loads and characteristics can evolve between the flying over of CALIPSO and Aqua or Terra. This is particularly crucial when the nocturnal orbits of CALIPSO are considered since AOD constraints are always provided by MODIS data acquired on daytime. Quantifying this effect requires to assess the evolution of AOD between MODIS-Aqua and MODIS-Terra. Furthermore, such a calculation does not take into account the possible bias on the MODIS-derived AOD. The existence of a systematic bias on MODIS-derived AOD can be highlighted using the sunphotometers of the AERONET network close to big cities in the Po valley.

3.2 Bias on the MODIS-derived AOD

Figure 2 shows an example of aerosol optical depth map at 550 nm derived from both MODISAqua (Fig. 2a) and MODIS-Terra (Fig. 2b) instruments over the Po Valley during a particularly high-polluted event on the 16 March 2007. This day is characterized by a high level of pollution due to anticyclonic conditions with a mean temperature of ~20 °C close to the surface. The weak southern wind (~6 $m\,s^{-1}$) sweeps pollutants northerly where they are stopped by the Alps and thus leads to higher AOD values in the northern part of the Po Valley (AOD larger than 1 near Venice). The mean AOD values derived from Aqua and Terra (with their variabilities) under CALIPSO track are 0.54(±0.15) and 0.47(±0.13), respectively. Although Aqua and Terra instruments are only separated by 1 h and 40 min, a significant evolution in the AOD pattern can be observed. Nevertheless, the mean values along the CALIPSO ground track are very similar within a margin of ~14%. Given that CALIOP and AquaMODIS instruments both belong to the A-Train constellation, their temporal coincidence is very good (~2 min). The temporal difference increases up to ~1 h and 40 min between CALIOP and Terra-MODIS. When CALIPSO orbit passes over the Po Valley at night-time, the MODIS-derived AODs obtained from daytime are the only ones that can be considered. This implies a temporal difference of about 11 h (resp. 9 h and 20 min) between CALIPSO and Aqua (resp. Terra). The atmospheric conditions may significantly evolve in such a time interval.

The bias on the AOD retrieved from MODIS at 550 nm has been assessed from a comparison with the AERONET sunphotometer at Ispra between June 2006 and November 2008 (Fig. 3). Data from the sun-photometer of Venice, located on the Acqua Alta Oceanographic Tower (AAOT) 8 nautical miles off the Venice Lagoon, have not been used because of subpixel water contamination in continental coastal regions (Chu et al., 2002). Hence, this station is not representative of the aerosol features found over the Po Valley. The sunphotometer-derived AOD at 550 nm have been interpolated using the Angström exponent (Angström, 1964) between 500 and 670 nm.

AMTD

3, 1323–1359, 2010

Synergy between CALIOP and MODIS instruments

P. Royer et al.

MODIS-derived AODs are computed using a weighted mean of pixels with a centre located at a distance lower than 10 km around Ispra station.

The agreement between MODIS-derived AOD and AERONET sunphometer-derived AOD is better when Aqua satellite is considered. The corresponding correlation coefficient is 0.89. Nevertheless, this value is associated with a mean bias of 0.047. When MODIS-Terra is considered, the correlation coefficient is 0.87 and the bias is larger (~0.088). When comparing τ_{MO} retrieved from MODIS-Terra and Aqua around Ispra station (Fig. 4) the previous biases are confirmed. MODIS-Terra slightly overestimates the AOD of 0.037 compared with MODIS-Aqua. Hereafter, biases have been applied to invert the mean CALIOP profiles assuming that sunphotometer-derived AODs are closer to the true values.

3.3 Uncertainties on BER

Major sources of uncertainties have been taken into account in order to assess both the standard deviation and the bias on the aerosol optical parameters retrieved from CALIOP/MODIS synergy. Uncertainty sources (i.e. the random detection processes and the error on τ_{MO}) have been supposed independent. The error budget on BER has been performed using a Monte Carlo method described in Chazette et al. (2002). The probability density functions of the uncertainty sources are supposed to follow a normal probability law with standard deviations associated to the SNR at each altitude level and to τ_{MO} (σ_{MO}). The sensitivity study on BER due to the uncertainty on the SNR (respectively on τ_{MO}) was thus performed using Monte Carlo simulations based on 1000 Gaussian random realizations of laser shots (resp. optical thicknesses) around the mean value of the SNR in the PBL (resp. of τ_{MO}). The results of the Monte Carlo approach involving various SNR values (inside the PBL) and different σ_{MO} are drawn in Fig. 5. The mean AOD at 550 nm has been chosen such as τ_{MO}=0.27 corresponding to the annual mean value measured over the Po Valley.

The averaged CALIOP level-1 profiles have a SNR ranging from 8 to 50 (Table 1) with a mean value of 18 leading to an uncertainty of ~0.001 sr^{-1} on BER retrieval. The uncertainty on MODIS-derived AODs (σ_{MO}) is comprised between 5 and 40% with a mean value of 17.5% corresponding to a BER uncertainty of ~0.002 sr^{-1}. According to Sect. 3.1, the uncertainty on BER due to RH effects is about 10% (~0.0013 sr^{-1}). The total uncertainty on BER retrieved from the synergy between CALIOP and MODIS instruments is thus ~0.003 sr^{-1}.

4 Results and discussion

4.1 MODIS-derived AOD over the Po Valley

A total of 102 and 104 coincidences between CALIOP and MODIS have been considered for Aqua and Terra, respectively. Figure 6 represents the temporal evolution of τ_{MO} computed from Aqua (Fig. 6a) and Terra (Fig. 6b) under CALIPSO ground track computed with Eq. 2.

A high variability of τ_{MO} is observed with a mean value close to 0.25. A seasonal cycle is clearly visible, mainly for MODIS-Terra, as already described by Mélin and Zibordi (2005) and Barnaba and Gobbi (2004). The lower AODs observed in winter and fall can be explained by an increase in precipitations involving a wet deposition removal and thus a decrease in the aerosol load. In summer, the high temperatures and a lack of precipitations contribute to increase the aerosol loads in the PBL. The mean annual AOD observed over the Po Valley (~0.27) is almost twice higher than that the one measured from sunphotometer observation over Paris, which is ~0.15 at 532 nm, as shown by Chazette et al. (2005). Other authors report similar mean values over great urban and industrial areas (e.g. Kim et al., 2007) found 0.33 at 550 nm over East Asia, Ramachandran (2007) 0.4 and 0.65 at 550 nm over Mumbai and New Delhi, Stammes and Henzing (2000) 0.26 at 501 nm over De Bilt (The Netherlands).

4.2 BER retrieved over the Po Valley

The algorithm described in Sect. 3.1 converges in 86 cases among 102 for MODIS-Aqua and 88 cases among 104 for MODIS-Terra. Among the 16 cases where the algorithm does not converge, 2 are night-time tracks and 12 have an AOD lower than 0.1. BER occurrences retrieved from this synergy are given in Fig. 7a and b. The classes of the histograms have been chosen accounting for the uncertainties on BER. The mean values of aerosol BER and extinction coefficient retrieved from CALIOP/MODIS-Aqua and Terra synergy and from CALIOP level-2 products are summarized in Table 2. The results are consistent between MODIS-Aqua and -Terra during both daytime and night-time. Indeed, mean BER and variabilities are close to 0.014(±0.003) sr^{-1} (LR=73 sr) and 0.013(±0.004) sr^{-1} (LR=78 sr) using MODIS-Aqua and Terra, respectively.

The CALIOP operational algorithm (level-2 products) gives access to vertical profile of BER with a resolution of 120 m every 40 km along CALIPSO track. The aerosol type is determined in each layer using a model-matching scheme (Vaughan, 2004a). The optical (attenuated backscatter coefficient at 532 nm, integrated attenuated total color ratio and depolarization ratio), geophysical (e.g. latitude, longitude) and temporal (season) characteristics are used to select the most likely BER for each layer. There are 6 different aerosols types (Vaughan, 2004b): polluted continental (BER∼0.014 sr^{-1}), biomass burning (BER∼0.014 sr^{-1}), desert dust (BER∼0.025 sr^{-1}), polluted dust (BER∼0.015 sr^{-1}), clean continental (BER∼0.029 sr^{-1}) and marine (BER∼0.050 sr^{-1}).

In order to compare BER retrieved from the spaceborne instrumental synergy CALIOP/MODIS with that derived from CALIOP operational algorithm, the latter needs to be integrated over the vertical column taking into account the relative weight of each aerosol layer in terms of extinction coefficient. The weighted BER is derived from the operational values of both the aerosol extinction (α_{ai}) and backscatter (β_{ai}) coefficients following the relation:

$$\mathrm{BER} = \frac{\sum_{i=1}^{N} \alpha_{\mathrm{ai}} \overbrace{\frac{\beta_{\mathrm{ai}}}{\alpha_{ai}}}^{\mathrm{BER}_i}}{\sum_{i=1}^{N} \alpha_{\mathrm{ai}}} \tag{4}$$

With the definition of BER_i, that leads to

$$\mathrm{BER} = \frac{\sum_{i=1}^{N} \beta_{\mathrm{ai}}}{\sum_{i=1}^{N} \alpha_{\mathrm{ai}}} \tag{5}$$

The subscript i=1 to N characterizes the altitude level in the CALIOP profile. The occurrences of BER derived from CALIOP operational product are also given in Fig. 7c. For all cases a more important weight on the calculation of BER is given to the lowest layers . We can notice a minimum threshold of ∼0.014 sr^{-1} (LR∼70 sr) corresponding to the minimum available value in the look-up table for polluted continental and biomass burning aerosols. The mean value and the variability of BER are close to 0.016(±0.003) sr^{-1} with an uncertainty of 30%. Such a value corresponds to either polluted continental or biomass burning or polluted dust aerosol models. Considering the uncertainties on BER retrieval, this mean value is not far from the one derived from the synergy between MODIS and CALIOP (0.013 sr^{-1}). The agreement between home-made and operational algorithms is better when using the synergy between CALIOP and MODIS-Aqua. Note that the bias observed between MODIS and the sunphotometer was smaller in this case. The lower BER retrieved from the coupling of CALIOP and MODIS are obviously derived from night-time lidar measurements.

AMTD

3, 1323–1359, 2010

BER retrieved here are typical for pollution aerosol emitted by traffic or industrial activities, which are the main sources of particulate pollution inside the Po valley (Table 1). Similar values have also been found for pollution aerosol type in the vicinity of big cities. Using surface measurements with a 180° backscatter nephelometer, Doherty et al. (1999) and Anderson et al. (2000) found BER∼0.015 sr^{-1} (LR∼60–70 sr) with an uncertainty of ∼20% in Washington State and ∼0.015(±0.001) sr^{-1} (LR∼64±4 sr) at the polluted continental site of Bondville in Illinois. Ansmann et al. (2001) found BER between ∼0.014 and ∼0.020 sr^{-1} (LR of 50–70 sr) for pollution from continental Europe from Raman lidar measurements at 532 nm at the Sagres island off the Portuguese coast during the Second Aerosol Characterization Experiment (ACE 2). Müller et al. (2001) have also take advantage of Raman lidar technique during INDOEX campaign to determine BER between ∼0.013 and ∼0.022 sr^{-1} (LR between 45 and 75 sr) from anthropogenic pollution including biomass burning emissions in India, whereas Chazette (2003) found BER values close to 0.030(±0.010) sr^{-1} (LR=33±11 sr) at 523 nm over the coastal site of Goa. Cattrall et al. (2005) found a mean BER of 0.014(±0.002) sr^{-1} (LR=71±10 sr) at 550 nm for urban/industrial aerosol type from AERONET sun-photometers measurements. Chazette et al. (2005) and Raut and Chazette (2007) used a synergy between lidar and sun-photometer in the framework of ESQUIF and LISAIR campaigns, respectively, to assess over Paris area BER between 0.013 and 0.017 sr^{-1} (LR between 59 and 77 sr) at 532 nm for aerosols mainly driven by traffic activities. Ground-based and airborne lidar systems have been used by Chazette et al. (2010) to determine the BER values and compare with CALIOP retrievals. They found a mean value of 0.026±0.002 sr^{-1} at 532 nm in the PBL much higher than CALIOP retrieval (∼0.020 sr^{-1}). This high discrepancy leads to an overestimation of aerosol extinction coefficient by a factor of 2. BER values lower than 0.015 sr^{-1} (LR higher than ∼67 sr) may come from biomass burning aerosols (e.g. Noh, 2008) whereas values higher than 0.020 sr^{-1} (lower than 50 sr) can be associated to sea salt or mineral dust aerosols. Pappalardo et al. (2004) found at 532 nm a LR of 40 sr and LR=56±7 sr (Pappalardo et al., 2010) and Catrall et al. (2005) ∼45 sr (0.022 sr^{-1})

over Sahara. Dust particles can be transported above Mediterranean Sea as described by Hamonou et al. (1999). Moreover, several dust events has been observed by Bonasoni et al. (2004) at Mt Cimone in the Italian northern Apennines. They may lead to an enhancement of BER when comparing to pollution aerosols.

The temporal evolutions of BER values is represented in Fig. 8. We can clearly notice a seasonal cycle with higher BER values during spring, summer and fall and lower values in winter. Such higher values (~0.020 sr^{-1}) can be explained by desert dust transport over the Po Valley, which occurred during these seasons as highlighted by backward trajectories performed using the Hysplit model (http://ready.arl.noaa.gov/HYSPLIT.php) and higher depolarization ratio values observed for BER value larger than 0.018 sr^{-1} (not shown).

4.3 Aerosol extinction coefficient retrieved over the Po Valley

We have also compared the vertical profiles of the aerosol extinction coefficient retrieved from the two methods: the MODIS/CALIOP synergy (α_{MO}) and the CALIOP level-2 operational algorithm. CALIOP level-1 data have been smoothed to obtain almost the same vertical resolution than CALIOP level-2 operational products. To quantify the differences distinguishing the two profiles, we have considered the mean square difference (Δ_αp in the PBL defined as:

$$\Delta_\alpha = \sqrt{\frac{1}{N_{PBL}} \sum_{i=1}^{N_{PBL}} (\alpha_{MO} - \alpha_{ai})^2} \tag{6}$$

where N_{PBL} is the number of CALIOP level-2 data in the PBL.

Two examples of aerosol extinction coefficient on the 15 September 2007 at 12:30 GMT and 8 September 2007 at 12:24 GMT are represented in Fig. 9a and b. In the first case, the two extinction coefficient profiles are in good agreement with mean square difference of 0.02 km^{-1} whereas a significant discrepancy can be observed in

AMTD
3, 1323–1359, 2010

Synergy between CALIOP and MODIS instruments

P. Royer et al.

the second example (mean square difference of 0.15 km^{-1}). In this last case, the integration of the CALIOP level-2 aerosol extinction profile gives an AOD of 0.16 compared with the value of 0.27 measured by MODIS-Aqua radiometer at the same time.

Occurrences of the mean square difference Δ_α are shown in Fig. 10a and b. The mean values of the distributions are 0.10 km^{-1} for MODIS-Aqua/CALIOP synergy and 0.13 km^{-1} for MODIS-Terra/CALIOP synergy. The AOD derived from the operational algorithm systematically underestimate the aerosol load, which demonstrates that the operational algorithm does not choose the good aerosol model.

5 Conclusion and perspectives

This paper fulfils the validation requirements of CALIOP operational algorithm over a polluted area. The synergy between CALIOP and MODIS instruments allowed retrieving aerosol optical properties over the Po Valley from June 2006 to February 2009. MODIS-derived aerosol optical depth at 550 nm (AOD) in the Po Valley showed a typical seasonal cycle with higher values on spring (0.29) and summer (0.30) and lower values during winter (0.22). On the same way, significant cycle on the backscatter-to-extinction ratio (BER) has been observed suggesting that the aerosol properties evolve during the year, mainly during both spring and summer where dust events occur. This is validated by the higher depolarisation ratio (not shown) observed at the same time. The mean BER retrieved from the synergy between the active spaceborne remote sensing instrument CALIOP and MODIS is ~0.014(±0.003) sr^{-1} for Aqua and ~0.013(±0.004) sr^{-1} for Terra, which is in good agreement with the mean value derived from the operational algorithm ~0.016(±0.003) sr^{-1}. These values are consistent to either polluted continental or biomass burning or polluted dust aerosol models. A mixing of different aerosol sources is probable. The operational algorithm does not necessarily choose the right aerosol model. The use of AODs from MODIS radiometers in synergy with CALIOP lidar could greatly improve the inversion and the retrieval of aerosol optical properties from space. This approach would deserve to be applied to other regions in order to assess the reliability of CALIOP operational algorithm on various aerosol types.

The synergy considered in this paper shows the potential of such an approach to survey large polluted area. The only one limitation is due to the signal to noise ratio that requires to average CALIOP profiles along the track on several tens of kilometres. Hence, the polluted area must cover a region larger than 100 km. The synergy between active and passive spaceborne instruments dedicated to the Earth survey promises an important development in the next decades. Such a synergy between CALIPSO/CALIOP and MODIS/Aqua or Terra is a powerful tool to apprehend the evolution of the Earth system influenced by human activities. Moreover, this study will be a great insight in the context of the validation of the further ADM-AEOLUS program scheduled to be launched at the end of 2011 (http://www.esa.int/esaLP/LPadmaeolus.html), which requires significant loads of particles to validate the Level 2 aerosol products.

Acknowledgements. This work was supported by the Comissariat à l'Energie Atomique (CEA) and the Centre National d'Etudes Spatiales (CNES). The authors would like to thank MODIS science data support team for processing level 2 data, and AERONET for collecting aerosol observations around the world and especially Giuseppe Zibordi the principal investigator of the Ispra site. CALIOP data were obtained from the NASA Langley Research Center Atmospheric Science Data Center (ASDC) via on-line web orders. We are very grateful to the entire CALIPSO science team for providing CALIOP data.

The publication of this article is financed by CNRS-INSU.

References

Anderson, T. L., Masonis, S. J., Covert, D. S., Charlson, R. J., and Rood, M. J.: In situ measurement of the aerosol extinction-to-backscatter ratio at a polluted continental site, J. Geophys. Res., 105(D22), 20907–20915, 2000.

Angström, A.: The parameters of atmospheric turbidity, Tellus, 16, 64–75, 1964.

Ansmann, A., Wandinger, U., Riebesell, M., Weitkamp, C., and Michaelis, W.: Independent measurement of extinction and backscatter profiles in cirrus clouds by using a combined Raman elastic-backscatter lidar, Appl. Optics, 31, 7113–7113, 1992.

Ansmann, A., Wagner, F., Althausen, D., Müller, D., Herber, A., and Wandinger, U.: European pollution outbreaks during ACE 2: Lofted aerosol plumes observed with Raman lidar at the Portuguese coast, J. Geophys. Res., 106(D18), 20725–20733, 2001.

Barnaba, F. and Gobbi, G. P.: Aerosol seasonal variability over the Mediterranean region and relative impact of maritime, continental and Saharan dust particles over the basin from MODIS data in the year 2001, Atmos. Chem. Phys., 4, 2367–2391, 2004, http://www.atmos-chem-phys.net/4/2367/2004/.

Berthier, S., Chazette, P., Couvert, P., Pelon, J., Dulac, F., Thieuleux, F., Moulin, C., and Pain, T.: Desert dust aerosol columnar properties over ocean and continental Africa from Lidar in-Space Technology Experiment (LITE) and Meteosat synergy, J. Geophys. Res., 111, D21202, doi:10.1029/2005JD006999, 2006.

Berthier, S., Chazette, P., Pelon, J., and Baum, B.: Comparison of cloud statistics from space-borne lidar systems, Atmos. Chem. Phys., 8, 6965–6977, 2008, http://www.atmos-chem-phys.net/8/6965/2008/.

Bonasoni, P., Cristofanelli, P., Calzolari, F., Bonafè, U., Evangelisti, F., Stohl, A., Zauli Sajani, S., van Dingenen, R., Colombo, T., and Balkanski, Y.: A erosol-ozone correlations during dust transport episodes, Atmos. Chem. Phys., 4, 1201–1215, 2004, http://www.atmos-chem-phys.net/4/1201/2004/.

Cattrall, C., Reagan, J., Thome, K., and Dubovik, O.: Variability of aerosol and spectral lidar and backscatter and extinction ratios of key aerosol types derived from selected Aerosol Robotic Network locations, J. Geophys. Res., 110, D10S11, doi:10.1029/2004JD005124, 2005.

AMTD

3, 1323–1359, 2010

Chazette, P., David, C., Lefrère, J., Godin, S., Pelon, J., and Mégie, G.: Comparative lidar study of the optical, geometrical, and dynamical properties of stratospheric post-volcanic aerosols, following the eruption of El Chichon and Mount Pinatubo, J. Geophys. Res., 100(D11), 23195–23207, 1995.

Chazette, P., Pelon, J., Moulin, C., Dulac, F., Carrasco, I., Guelle, W., Bousquet, P., and Flamant, P. H.: Lidar and satellite retrieval of dust aerosols over the azores during SOFIA/ASTEX. Atmos. Environ. 35, 4297–4304, 2001.

Chazette, P., Pelon, J., and Mégie, G.: Determination by spaceborne backscatter lidar of the structural parameters of atmospheric scattering layers, Appl. Optics, 40, 3428–3440, 2002.

Chazette, P.: The monsoon aerosol extinction properties at Goa during INDOEX as measured with lidar, J. Geophys. Res., 108(D6), 4187, doi:10.1029/2002JD002074, 2003.

Chazette, P., Randriamiarisoa, H., Sanak, J., Couvert P., and Flamant, C.: Optical properties of urban aerosol from airborne and ground-based in situ measurements performed during the ESQUIF program, J. Geophys. Res, 110(D2), D02206, doi:10.1029/2004JD004810, 2005.

Chazette, P., Sanak, J., and Dulac, F.: New Approach for Aerosol Profiling with a Lidar Onboard an Ultralight Aircraft: Application to the African Monsoon Multidisciplinary Analysis, Environ. Sci. Technol., 41(24), 8335–8341, doi:10.1021/es070343y, 2007.

Chazette, P., Raut, J.-C., Dulac, F., Berthier, S., Kim, S.-W., Royer, P., Sanak, J., Loaëc, S., and Grigaut-Desbrosses, H.: Simultaneous observations of lower tropospheric continental aerosols with a ground-based, an airborne, and the spaceborne CALIOP lidar systems, J. Geophys. Res., Special issue on CALIPSO data, doi:10.1029/2009JD012341, in press, 2010.

Chu, D. A., Kaufman, Y. J., Ichoku, C., Remer, L. A., Tanré, D., and Holben, B. N.: Validation of MODIS aerosol optical depth retrieval over land, Geophys. Res. Lett., 29(12), 8007, doi:10.1029/2001GL013205, 2002.

Doherty, S. J., Anderson, T. L., and Charlson, R. J.: Measurement of the lidar ratio for atmospheric aerosol with a 180° backscatter nephelometer, Appl. Optics, 38, 1823–1832, 1999.

Dockery, D. and Pope, A.: Epidemiology of acute health effects: summary of time-series, in: Particles in Our Air: Concentration and Health Effects, edited by: Wilson, R. and Spengler, J. D., Harvard University Press, Cambridge, MA, USA, 123–147, 1996.

Dulac, F. and Chazette, P.: Airborne study of a multi-layer aerosol structure in the eastern Mediterranean observed with the airborne polarized lidar ALEX during a STAAARTE campaign (7 June 1997), Atmos. Chem. Phys., 3, 1817–1831, 2003, http://www.atmos-chem-phys.net/3/1817/2003/.

Hamonou, E., Chazette, P., Balis, D., Dulac, F., Schneider, X., Galani, E., Ancellet, G., and Papayannis, A.: Characterisation of the vertical structure of Saharan dust export to the Mediterranean basin, J. Geophys. Res., 18, 2257–2270, 1999.

Haywood, J. M., Pelon, J., Formenti, P., Bharmal, N., Brooks, M., Capes, G., Chazette, P., Chou, C., Christopher, S., Coe, H., Cuesta, J., Derimian, Y., Desboeufs, K., Greed, G., Harrison, M., Heese, B., Highwood, E. J., Johnson, B., Mallet, M., Marticorena, B., Marsham, J., Milton, S., Myhre, G., Osborne, S. R., Parker, D. J., Rajot, J.-L., Schultz, M., Slingo, A., Tanré, D., and Tulet, P.: Overview of the dust and biomass-burning experiment and African Monsoon Multidisciplinary Analysis special observing period-0, J. Geophys. Res., 113, D00C17, doi:10.1029/2008JD010077, 2008.

Highwood, E. J., Haywood, J. M., Coe, H., Cook, J., Osborne, S., Williams, P., Crosier, J., Formenti, P., McQuaid, J., Brooks, B., Thomas, G., Grainger, R., Barnaba, F., Gobbi, G. P., and De Leeuw, G.: Aerosol Direct Radiative Impact Experiment (ADRIEX) overview., Q. J. Roy. Meteor. Soc., 133(S1), 3–15, 2007.

Holben, B. N., Eck, T. F., Slutsker, I., Tanré, D., Buis, J. P., Setzer, A., Vermote, E., Reagan, J. A., Kaufman, Y., Nakajima, T., Lavenu, F., Jankowiak, I., and Smirnov, A.: AERONET – A federated instrument network and data archive for aerosol characterization., Rem. Sens. Environ., 66, 1–16, 1998.

Klett, J. D.: Stable analytical inversion solution for processing lidar returns, Appl. Optics., 20, 211–220, 1981.

King, M. D., Kaufman, Y. J., Menzel, W. P., and Tanre, D.: Remote sensing of cloud, aerosol, and water vapor properties from the Moderate Resolution Imaging Spectrometer (MODIS), IEEE T. Geosci. Remote, 30(1), 2–27, 1992.

Kim, S.-W., Yoon, S.-C., Kim, J., and Kim, S.-Y.: Seasonal and monthly variations of columnar aerosol optical properties over east Asia determined from multi-year MODIS, LIDAR and AERONET Sun/sky radiometer measurements, Atmos. Environ., 41, 1634–1651, 2007.

Kim, S.-W., Berthier, S., Raut, J.-C., Chazette, P., Dulac, F., and Yoon, S.-C.: Validation of aerosol and cloud layer structures from the space-borne lidar CALIOP using a ground-based lidar in Seoul, Korea, Atmos. Chem. Phys., 8, 3705–3720, 2008, http://www.atmos-chem-phys.net/8/3705/2008/.

Laaksonen, A., Hamed, A., Joutsensaari, J., Hiltunen, L., Cavalli, F., Junkermann, W., Asmi, A., Fuzzi, S., and Facchini, M. C.: Cloud condensation nucleus production from nucleation events at a highly polluted region, Geophys. Res. Lett., 32, L06812, doi:10.1029/2004GL022092, 2005.

Lauwerys, R. R. : Toxicologie industrielle et intoxications professionnelles, Masson, 1982.

Lawrence, M. G., Butler, T. M., Steinkamp, J., Gurjar, B. R., and Lelieveld, J.: Regional pollution potentials of megacities and other major population centers, Atmos. Chem. Phys., 7, 3969–3987, 2007, http://www.atmos-chem-phys.net/7/3969/2007/.

Measures, R. M.: Laser remote sensing: Fundamentals and Applications, Wiley and Sons, New York, 1984.

Mélin, F. and Zibordi, G.: Aerosol variability in the Po Valley analyzed from automated optical measurements, Geophys. Res. Lett., 32, L03810, doi:10.1029/2004GL021787, 2005.

Müller, D., Franke, K., Wagner, F., Althausen, D., Ansmann, A., Heintzenberg, J., and Verver, G.: Vertical profiling of optical and physical particle properties over the tropical Indian Ocean with six-wavelength lidar 2. Case studies, J. Geophys. Res., 106(D22), 28577–28595, 2001.

Neftel, A., Spirig, C., Prevot, A. S. H., Furger, M., Stutz, J., Vogel, B., and Hjorth, J.: Sensitivity of photooxidant production in the Milan Basin: An overview of results from a EUROTRAC-2 Limitation of Oxidant Production field experiment, J. Geophys. Res., 107, 8188, doi:10.1029/2001JD001263, 2002.

Noel, V., Hertzog, A., Chepfer, H., and Winker, D. M.: Polar stratospheric clouds over Antarctica from the CALIPSO spaceborne lidar, J. Geophys. Res., 113, D02205, doi:10.1029/2007JD008616, 2008.

Noh, Y. M., Kim, Y. J., and Müller, D.: Seasonal characteristics of lidar ratios measured with a Raman lidar at Gwangju, Korea in spring and autumn, Atmos. Environ., 42, 2208–2224, 2008.

Pappalardo, G., Amodeo, A., Pandolfi, M., Wandinger, U., Ansmann, A., Bösenberg, J. J., Matthias, V., Amiridis, V., De Tomasi, F., Frioud, M., Iarlori, M., Komguem, L., Papayannis, A., Rocadenbosch, F., and Wang, X.: Aerosol Intercomparison in the Framework of the EARLINET Project. 3. Raman lidar algorithm for aerosol extinction, backscatter, and lidar ratio, Appl. Optics, 43(28), 5370–5385, 2004.

Pappalardo, G., Wandinger, U., Mona, L., Hiebsch, A., Mattis, I., Amodeo, A., Ansmann, A., Seifert, P., Linne, H., Apituley, A., Alados Arboledas, L., Balis, D., Chaikovsky, A., D'Amico, G., De Tomasi, F., Freudenthaler, V., Giannakaki, E., Giunta, A., Grigorov, I., Iarlori, M., Madonna, F., Mamouri, R.-E., Nasti, L., Papayannis, A., Pietruczuk, A., Pujadas, M., Rizi, V., Rocadenbosch, F., Russo, F., Schnell, F., Spinelli, N., Wang, X., and Wiegner, M.: EARLINET correlative measurements for CALIPSO: First intercomparison results, J. Geophys. Res., doi:10.1029/2009JD012147, accepted, 2009.

Pelon, J., Flamant, C., Chazette, P., Léon, J. F., Tanré, D., Sicard, M., and Satheesh, S. K.: Characterization of aerosol spatial distribution and optical properties over the Indian Ocean from airborne lidar and radiometry during INDOEX'99, J. Geophys. Res., 107(D19), 8029, doi:10.1029/2001JD000402, 2002.

Petritoli, A., Bonasoni, P., Giovanelli, G., Ravegnani, F., Kostadinov, I., Bortoli, D., Weiss, A., Schaub, D., Richter, D., and Fortezza, F.: First comparison between ground-based and satellite-borne measurements of tropospheric nitrogen dioxide in the Po basin, J. Geophys. Res., 109, D15307, doi:10.1029/2004JD004547, 2004.

Ramachandran, S.: Aerosol optical depth and fine mode fraction variations deduced from Moderate Resolution Imaging Spectroradiometer (MODIS) over four urban areas in India, J. Geophys. Res., 112, D16207, doi:10.1029/2007JD008500, 2007.

Raut, J.-C. and Chazette, P.: Retrieval of aerosol complex refractive index from a synergy between lidar, sunphotometer and in situ measurements during LISAIR experiment, Atmos. Chem. Phys., 7, 2797–2815, 2007, http://www.atmos-chem-phys.net/7/2797/2007/.

Raut, J.-C. and Chazette, P.: Vertical profiles of urban aerosol complex refractive index in the frame of ESQUIF airborne measurements, Atmos. Chem. Phys., 8, 901–919, 2008a, http://www.atmos-chem-phys.net/8/901/2008/.

Raut, J.-C. and Chazette, P.: Radiative budget in the presence of multi-layered aerosol structures in the framework of AMMA SOP-0, Atmos. Chem. Phys., 8, 6839–6864, 2008b, http://www.atmos-chem-phys.net/8/6839/2008/.

Salmonson, V. V., Barnes, W. L., Maymon, P. W., Montgomery, H. E., and Ostrow, H.: MODIS: Advanced Facility Instrument for Studies of the Earth as a System, IEEE Trans. Geosci. Remote, 27, 145–153, 1989.

Sassen, K., Wang, Z., and Liu, D.: Global distribution of cirrus clouds from CloudSat/Cloud-Aerosol Lidar and Infrared Pathfinder Satellite Observations (CALIPSO) measurements, J. Geophys. Res., 113, D00A12, doi:10.1029/2008JD009972, 2008

Sicard, M., Chazette, P., Pelon, J., Won, J. G., and Yoon, S.-C.: Variational method for the retrieval of the optical thickness and the backscatter coefficient from multiangle lidar profiles, Appl. Optics, 41, 493–502, 2002.

Stammes, P. and Henzing, J.: Multispectral aerosol optical thickness at De Bilt 1997–1999, J. Aerosol Sci., 31, 283–284, 2000.

Stephens, G. L., Vane, R. J., Boain, R. J., Mace, G. G., Sassen, K., Wang, Z. E., Illingworth, A. J., O'Connor, E. J., Rossow, W. B., Durden, S. L., Miller, S. D., Austin, R. T., Benedetti, A., and Mitrescu, C.: The CloudSat mission and the A-Train: A new dimension of space-based observations of clouds and precipitation, Bull. Am. Meteorol. Soc., 83, 1771–1790, 2002.

Thomason, L. W., Pitts, M. C., and Winker, D. M.: CALIPSO observations of stratospheric aerosols: a preliminary assessment, Atmos. Chem. Phys., 7, 5283–5290, 2007, http://www.atmos-chem-phys.net/7/5283/2007/.

Vaughan, M. A., Young, S. A., Winker, D. M., Powell, K. A., Omar, A. H., Liu, Z., Hu, Y., and Hostetler, C. A.: Fully automated analysis of space-based lidar data: An overview of the CALIPSO retrieval algorithms and data products, Proc. SPIE, 5575, 16–30, doi:10.1117/12.572024, 2004a.

Vaughan, M.: Algorithm for retrieving lidar ratios at 1064 nm from space-based lidar backscatter data, Proc. SPIE, 5240, 104–115, 2004b.

Winker, D. M., Pelon, J., and McCormick, M. P.: The CALIPSO mission: Spaceborne lidar for observation of aerosols and clouds, Proc. SPIE, 4893, 1–11, 2003.

Table 1. Seasonal and spatial distributions of CALIOP level-1 data in cloud-free conditions over the Po Valley from June 2006 to February 2009. The nearest big cities flew over by CALIPSO are given with their numbers of inhabitants and the main aerosol sources. The mean number of profiles and the corresponding SNR in the PBL are also specified for each orbit.

Seasons		Milan	Turin	Genoa	Bologna	Venice	Trente	Total
2006	JJA	2	1	3	–	3	3	12
	SON	4	0	4	–	0	2	10
2007	DJF	3	1	1	–	2	3	10
	MAM	3	0	2	–	4	4	13
	JJA	1	1	1	–	3	5	11
	SON	3	1	1	–	4	5	14
2008	DJF	5	0	3	–	6	3	17
	MAM	1	1	1	–	1	0	4
	JJA	3	1	1	–	1	4	10
	SON	3	0	2	–	5	1	11
2009	DJF	2	1	2	–	3	1	9
Total		30	7	21	–	32	31	121
Number of inhabitants		750 000	2 200 000	880 000	375 000	270 000	115 000	4 590 000
Main sources of aerosols		traffic textile mech. chemical w.&p. meta.	traffic mech. textile chemical w.&p. meta.	traffic mech. textile chemical meta.	traffic mech. chemical building material	textile meta. chemical, buildings	mech. meta.	
Number of profiles	day	197(±33)	–	157(±43)	–	152(±33)	316(±77)	210(±46)
	night	184(±35)	81(±45)	–	–	446(±112)	223(±62)	234(±63)
SNR	day	14(±4)	–	12(±3)	–	12(±3)	16(±4)	14(±3)
	night	23(±4)	13(±3)	–	–	35(±4)	25(±6)	24(±4)

mech. = mechanical; w.&p. = wood and paper; meta. = metallurgical.

AMTD

3, 1323–1359, 2010

Table 2. Mean value and variability on aerosol BER and extinction coefficient in the PBL retrieved from CALIOP/MODIS-Aqua and Terra synergies and from CALIOP level-2 products.

	BER (sr^{-1})			Aerosol extinction coefficient (km^{-1})		
data	CALIOP/ MODIS-Aqua	CALIOP/ MODIS-Terra	CALIOP level-2	CALIOP/ MODIS-Aqua	CALIOP/ MODIS-Terra	CALIOP level-2
day	0.015(±0.002)	0.014(±0.003)	0.016(±0.003)	0.21(±0.10)	0.24±(0.12)	0.14±(0.08)
night	0.012(±0.004)	0.011(±0.004)	0.016(±0.002)	0.17(±0.06)	0.22±(0.08)	0.12±(0.06)
all	0.014(±0.003)	0.013(±0.004)	0.016(±0.003)	0.20(±0.09)	0.23±(0.10)	0.13±(0.07)

AMTD

3, 1323–1359, 2010

Synergy between CALIOP and MODIS instruments

P. Royer et al.

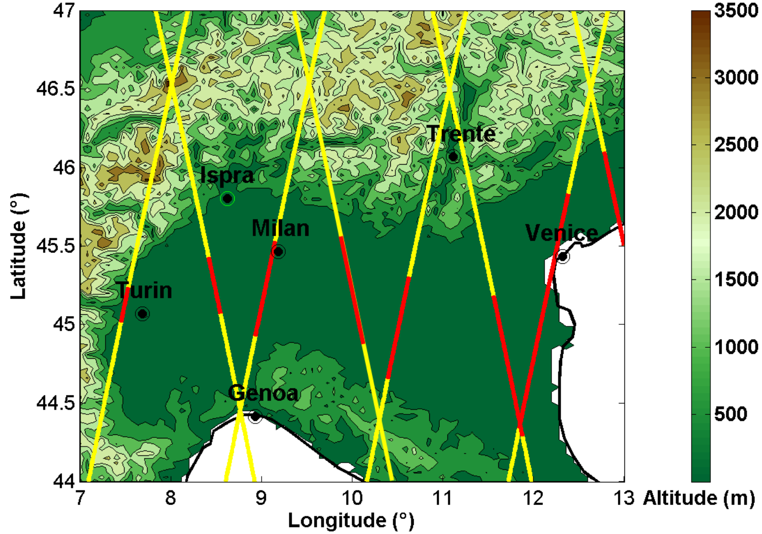

Fig. 1. Main cities and topography of the Po Valley region. The yellow solid lines represent the ground-tracks of CALIPSO orbits that have been considered. The red sections highlight the useful part of the orbits with a mean sea level (MSL) altitude lower than 0.2 km.

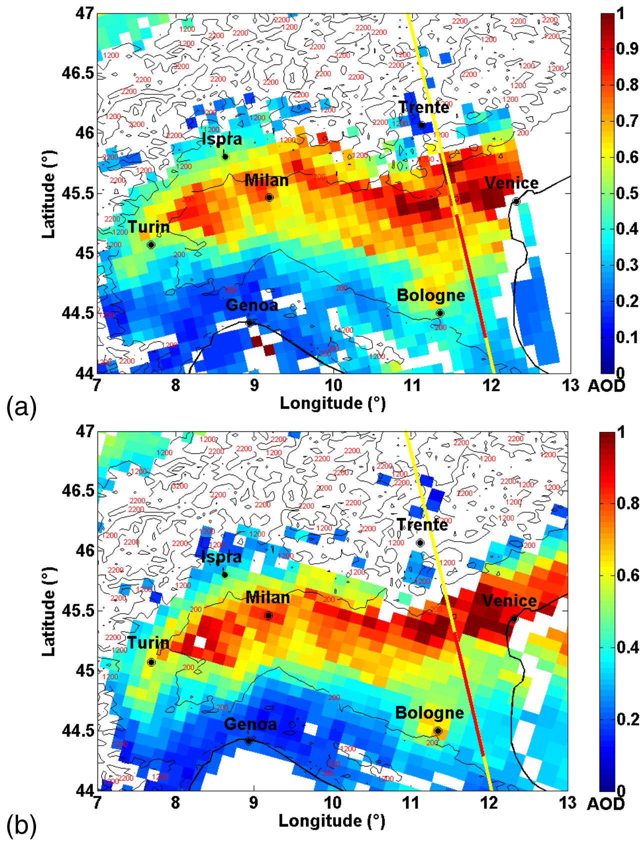

Fig. 2. AOD map at 550 nm over the Po Valley on the 16 March 2007 from **(a)** MODIS-Aqua at 12:20 UTC and **(b)** MODIS-Terra at 10:40 UTC. The topography levels around the Po valley are shown in black lines. The yellow solid line represents the ground-track of CALIPSO orbits that have been considered and the red section highlights the useful part of the orbits with an altitude lower than 0.2 km a.m.s.l.

AMTD

3, 1323–1359, 2010

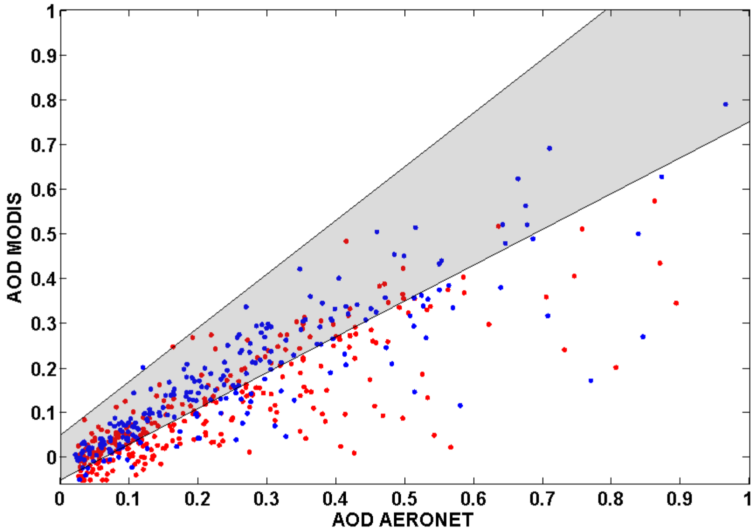

Fig. 3. Comparison of AOD values between June 2006 and November 2008 retrieved from MODIS-Terra (249 blue dots) and Aqua (210 red dots) instruments at 550 nm, and Ispra AERONET sun-photometer. The sunphotometer-derived AODs τ_{MO} at 550 nm have been calculated using the Angström exponent between 500 and 675 nm. The gray shaded area represents the standard deviation $\sigma_{MO} = \pm 0.05 \pm 0.2\ \tau_{MO}$ on MODIS radiometers.

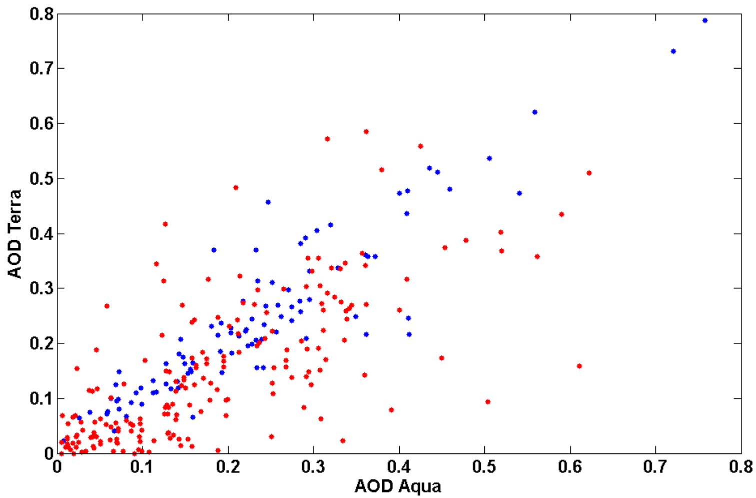

Fig. 4. Intercomparison of the mean MODIS-derived AODs along the CALIPSO tracks (96 blue dots) and near Ispra site (233 red dots) when considering Terra and Aqua platforms.

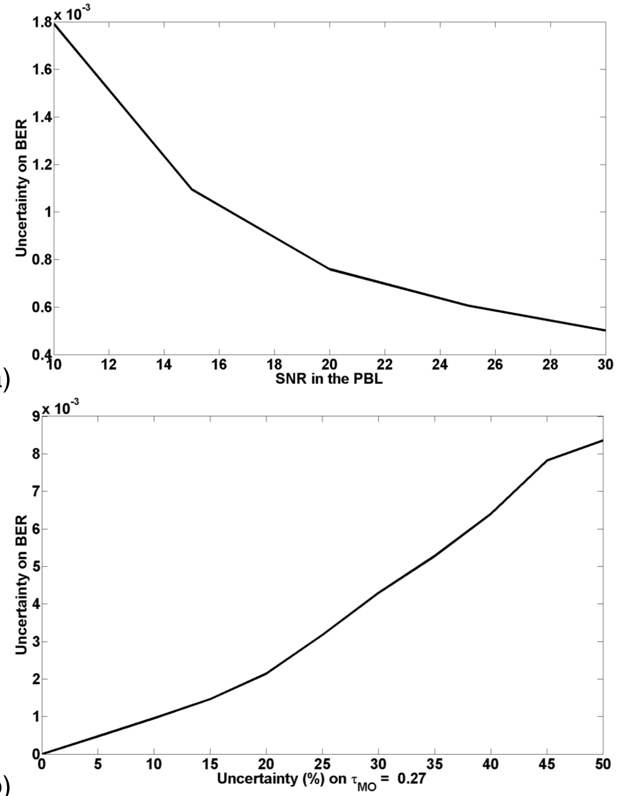

(a)

(b)

Fig. 5. Results of Monte Carlo simulations to assess the uncertainty on BER retrieval **(a)** due to the SNR in the PBL of the lidar range-corrected signal and **(b)** due to the uncertainty on MODIS-derived AODs (σ_{MO}) for a mean value τ_{MO}=0.27.

AMTD

3, 1323–1359, 2010

Title Page
Abstract | Introduction
Conclusions | References
Tables | Figures
◂ | ▸
Back | Close
Full Screen / Esc
Printer-friendly Version
Interactive Discussion

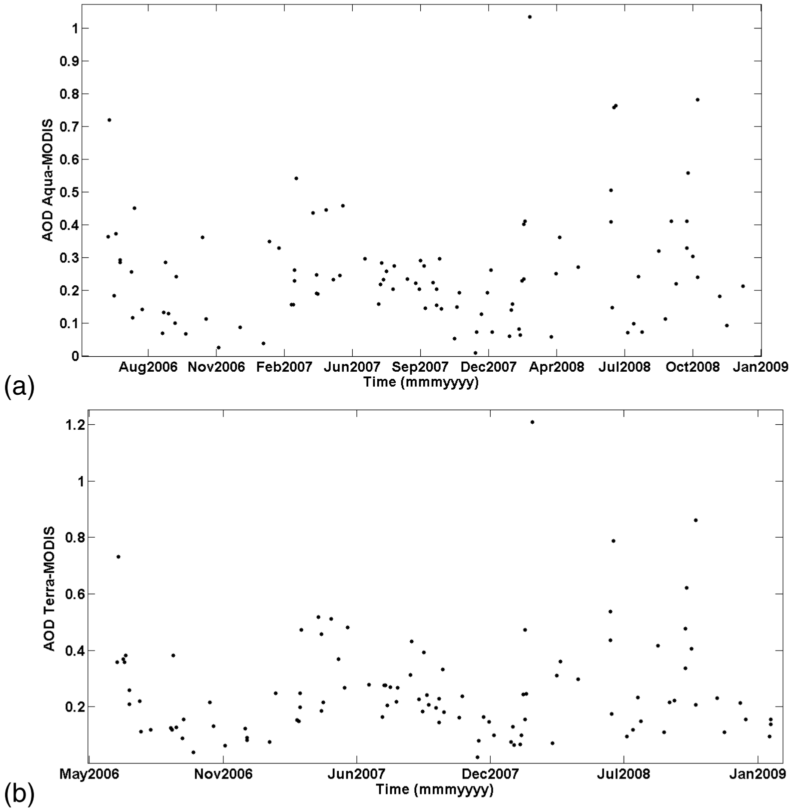

Fig. 6. Temporal evolution of the mean AOD at 550 nm (τ_{MO}) under CALIPSO ground track between June 2006 and February 2009 from **(a)** MODIS-Aqua (102 data) and **(b)** MODIS-Terra (104 data) for the situations where both CALIOP and MODIS data are available.

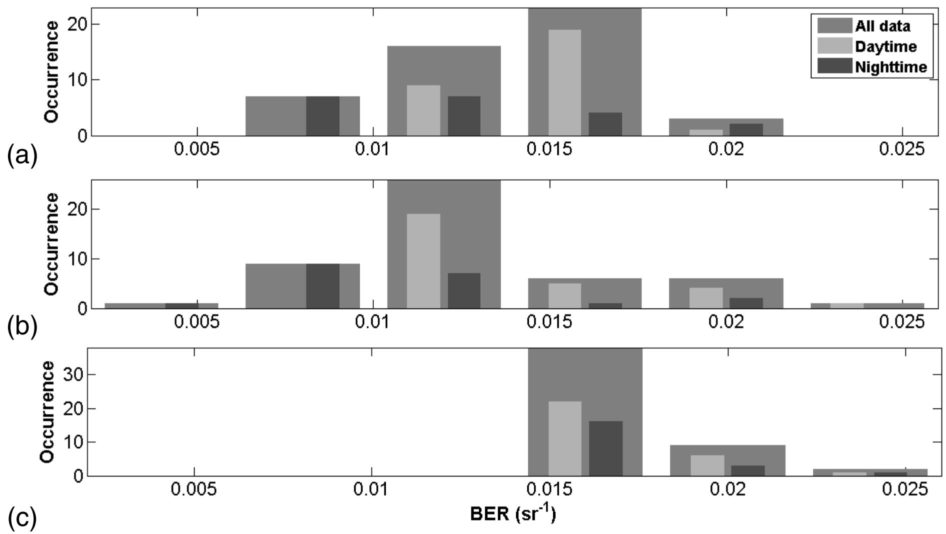

Fig. 7. Occurrences for coincident aerosol BER values (49 data) from **(a)** CALIOP/MODIS-Aqua synergy, **(b)** CALIOP/MODIS-Terra synergy and **(c)** operational products of CALIOP level-2 for daytime (light gray), night-time (black) and all data (dark gray).

AMTD
3, 1323–1359, 2010

Title Page
Abstract | Introduction
Conclusions | References
Tables | Figures
Back | Close
Full Screen / Esc
Printer-friendly Version
Interactive Discussion

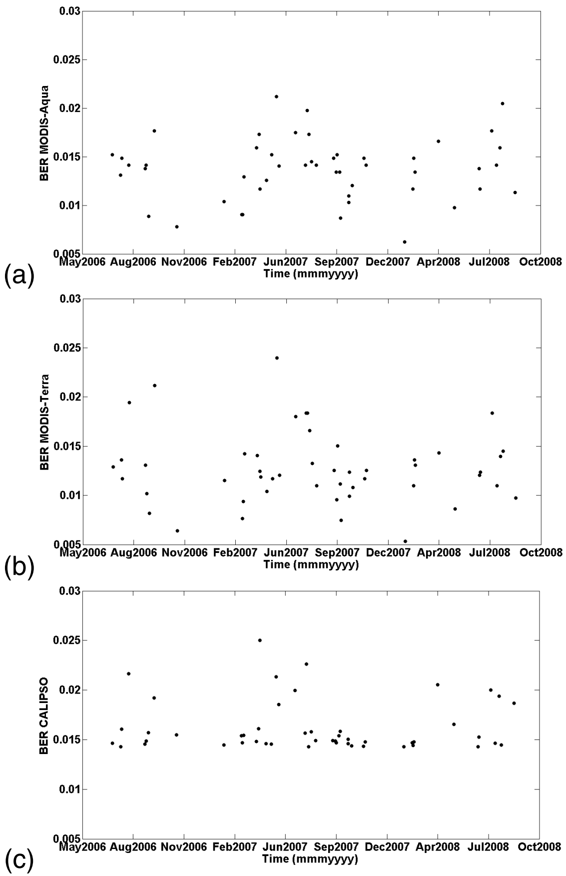

Fig. 8. Temporal evolution from June 2006 to February 2009 of BER values (49 data) over the Po Valley from **(a)** CALIOP/MODIS-Aqua synergy, **(b)** CALIOP/MODIS-Terra synergy and **(c)** CALIOP level-2 products.

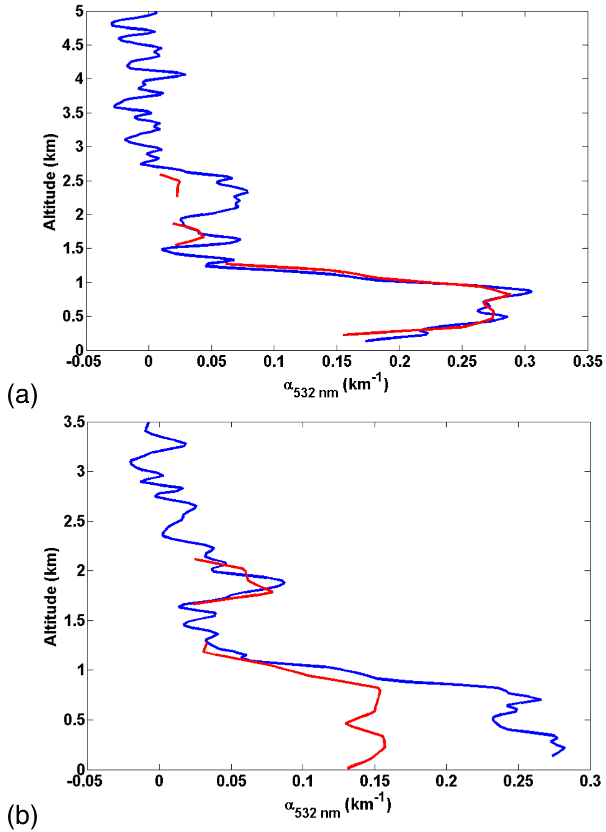

Fig. 9. Mean vertical profiles of aerosol extinction coefficient at 532 nm on **(a)** 15 September 2007 at 12:30 GMT and **(b)** 8 September 2007 at 12:24 GMT. The aerosol extinction coefficient is obtained from CALIOP level-2 operational product (red line) and from CALIOP level-1 data inverted with the aerosol BER retrieved from the synergy with MODIS (blue line).

AMTD

3, 1323–1359, 2010

Synergy between CALIOP and MODIS instruments

P. Royer et al.

Title Page
Abstract | Introduction
Conclusions | References
Tables | Figures
◄| |►
◄ ►
Back | Close
Full Screen / Esc
Printer-friendly Version
Interactive Discussion

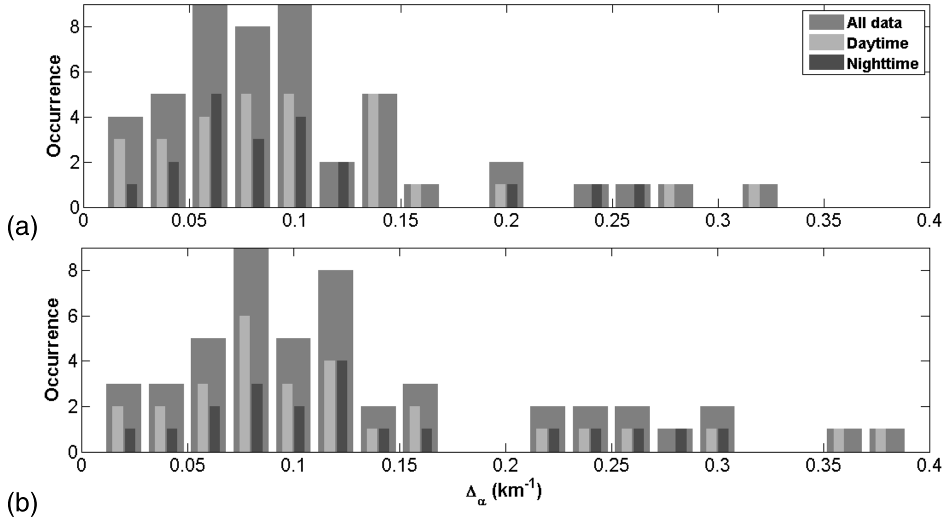

Fig. 10. Occurrence of the mean square difference in the PBL (Δ_αp b etween extinction coefficient from **(a)** CALIOP level-2 and MODIS-Aqua/CALIOP synergy and **(b)** CALIOP level-2 and MODIS-Terra/CALIOP synergy for daytime (light gray), night-time (black) and all data (dark gray).